Macromolecules

Article

Cite This: Macromolecules 2018, 51, 2187−2194

pH-Dependent Conformations for Hyperbranched Poly(ethylenimine) from All-Atom Molecular Dynamics

In Kim,[†] Tod A. Pascal,[‡] Seong-Jik Park,[⊥] Mamadou Diallo,[†] William A. Goddard III,[*,§] and Yousung Jung[*,†]

[†]Graduate School of Energy, Environment, Water and Sustainability (EEWS), Korea Advanced Institute of Science and Technology, Daejeon 34141, Korea

[‡]The Molecular Foundry, Lawrence Berkeley National Laboratory, Berkeley, California 94720, United States

[⊥]Department of Bioresources and Rural Systems Engineering, Hankyong National University, Kyonggi 17579, South Korea

[§]Materials and Process Simulation Center, Division of Chemistry and Chemical Engineering, California Institute of Technology, Pasadena, California 91125, United States

Supporting Information

ABSTRACT: Hyperbranched poly(ethylene imine) (PEI) with its high amino content is a versatile functional polymer that is widely used as a gene delivery vector in biological applications and as a ligand and precursor for ion exchange resins and membranes in water purification and metal recovery. We report here the first fully atomistic model of a 25 kDa hyperbranched PEI macromolecule. We utilized this model to carry out molecular dynamics (MD) simulations with explicit water molecules and chloride ions to study pH-dependent conformational changes. We find that growing the PEI macromolecule sequentially from the monomers yields atomistic structures whose sizes (radius of gyration) are in good agreement with the small angle neutron scattering experiments. Our analysis of the structural properties from MD simulations shows that conformations of the hyperbranched PEI exhibit oblate ellipsoidal elongation at low pH compared to high or neutral pH but with no significant changes in the corresponding sizes. This fully atomistic model of a 25 kDa hyperbranched PEI macromolecule in water provides much needed detailed atomistic information for advancing our fundamental understanding of the structures and host−guest properties of PEI-based functional reagents and materials for biomedical and sustainability related applications.

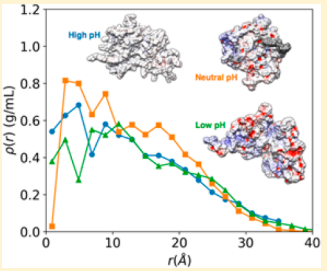

1. INTRODUCTION

Hyperbranched polymers have emerged over the past decade as promising materials for a wide range of novel nanomaterials applications.[1−3] With their versatile functionality combined with suitable nm-sized dimensions and cost-effective synthesis procedures, hyperbranched polymers have received much attention as alternatives to dendrimers. Poly(ethylene imine) (PEI), which can be synthesized as a hyperbranched or linear polymer, is a well-known commercial macromolecule that has been used extensively in a variety of applications.[4,5] Due to its high content of amino groups, hyperbranched PEI has been applied recently as a gene delivery vector[6−8] and as a precursor for the preparation of high capacity anion exchange resins and ion selective membranes.[9−13] Generally, the conformations of a hyperbranched polymer play an important role in the applications. For example, protonated PEI become highly cationic in acidic conditions, forming PEI/DNA complexes with nucleic acids suitable for utilization as gene delivery system in physiological conditions.[5,14−17] In addition, changing the pH can alter the conformation and hence the flux and permselectivity of membranes with PEI-based separation layers.[18,19] This shape change offers the opportunity for the formation of more open and porous separation layers in PEI-based ion selective membranes. In both cases, the conformational responsive to pH provides insights into the atomistic structure and properties important in the applications. Thus, understanding the polymer equilibrium structure and the solvation structure are essential. Indeed, Liu et al.[20] recently carried out atomistic MD simulations on a generation 4 (G4-NH_2) polyamidoamine (PAMAM) dendrimer as a function of pH and showed that the conformation changes dramatically with the degree of protonation from a dense-core at high pH to a dense-shell structure at low pH upon. Such changes can have profound effects on the host−guest properties of branched macromolecules including drug delivery mechanisms.

Despite the great potential and widespread usage of hyperbranched polymers as functional materials, their polydispersity[4] has hindered detailed experimental studies so that little is known of the atomistic structure and conformations of hyperbranched polymers.[7,21] Compared to dendrimers, hyperbranched polymers are generally easy to synthesize in one-step on a large scale, however, this "one-step" procedure usually leads to uncontrolled statistical growth in molecular weight (MW) and degree of branching.[22,23] After the first report on

Received: December 4, 2017
Revised: February 20, 2018
Published: March 6, 2018

Downloaded via UNIV OF CALIFORNIA SAN DIEGO on March 26, 2021 at 01:01:41 (UTC).
See https://pubs.acs.org/sharingguidelines for options on how to legitimately share published articles.

© 2018 American Chemical Society

DOI: 10.1021/acs.macromol.7b02573
Macromolecules 2018, 51, 2187−2194

hyperbranched polymers by Aerts,[24] a number of synthesis models and relationships between the topology and static properties were investigated[25−30] with the help of computer simulations. These theoretical studies have led to two conventional models for hyperbranched polymer growth:

- The "**quick growth**" model which leads to cluster−cluster aggregation and formation of a larger polymer network and
- The "**slow growth**" model which mimics a sequential growth process of a ring-opening polymerization of aziridine, the functional reagent that is utilized in the industrial scale synthesis of hyperbranched PEI.

It is known that the two models lead to quite different topologies with different local structures at a coarse-grained level.[31] This diversity in the topological domain makes the atomistic modeling of a hyperbranched polymers more complicated than that of a dendrimer, which has a well-defined molecular architecture at a given composition. Indeed, very few computational studies have been performed on hyperbranched PEI macromolecules despite their widespread utilization as functional materials in biomedical and sustainability related applications. Ziebarth and Wang studied titration curves of a 20-mer linear PEI using all-atom Monte Carlo simulations.[32] Choudhury and Roy performed a conformational analysis and solvation dynamics of a 20-mer and 50-mer PEI chains.[16] They observed the conformational changes, local structuring, and dynamical changes in solvation shells of linear PEIs as pH was varied. Sun et al. carried out molecular dynamics simulations of PEI/DNA complexes with explicit water and counterions to probe the effect of protonation DNA binding to PEI.[6] They concluded that the protonation states are more influential than the degree of branching of the polymer. However, only a few cases with branching and with only a low-molecular weight (LMW)-PEI were studied. Poghoshan et al. carried out MD simulations of hyperbranched PEI inside inverse micelles formed in heptanol.[33] They reported a change in the size of the polymer within the surfactant micelles though it is unclear how they built and connected the starting 3-D atomistic model of their hyperbranched PEI macromolecule.

To provide a detailed and consistent understanding of the structures and properties of hyperbranched PEI, it is important to build an atomistic model of the structure in the same way that it would be branched experimentally. To date, there is no precise understanding of the atomistic structure of hyperbranched PEI in water. Indeed, almost all studies related to hyperbranched polymers have been focused on modeling random structures, with very few studies considering hyperbranched polymers and changes in pH with explicit salt ions.

In this work, we perform molecular dynamics(MD) simulations with fully atomistic hyperbranched PEI macromolecules to study how their conformation changes as a function of pH. Methodologically, we find that, for hyperbranched PEI, the **sequential growth (SG)** method yields a proper power law, which is a more realistic atomistic structure than from the **quick growth (QG)** method. We also examine here how the structural properties of the hyperbranched PEIs (radial density profiles, shapes, radial distribution functions, radius of gyration, solvent accessible surface area, and electrostatic potential surface) depend on the protonation level for three different experimentally proposed pH regions. The overall results of our atomistic MD simulations are consistent with experiments[21] and show that a 25 kDa hyperbranched PEI macromolecule undergoes conformational changes with elongation in one direction at low pH.

2. MODEL AND SIMULATIONS METHODS

We used Monte Carlo techniques to generate random hyperbranched PEI model structures with a molar mass of 25 kDa and primary, secondary, and tertiary amine molar contents of 25%, 50%, and 25%, respectively, consistent with the experimental data[34] and polymer growth procedure. It is worth mentioning that commercially available PEIs having a specified molecular weight are generally polydisperse.[35] However, to simplify the number of parameters to be considered, we considered here the monodisperse case.

Figure 1 highlights the methodology that we used to generate the atomistic model of our hyperbranched PEI. First, we built a coarse-grained model that contains the overall connection information between monomers. The total number of monomers n in one hyperbranched polymer is determined by dividing the molecular weight of the target molecule by the molecular weight of monomer. In this work, we chose the target as hyperbranched PEI with 25 kDa. Since the molecular weight of ethylamine monomer is Mw = 45.08 g/mol, we need n = 580 monomers per chain (with an average of two H atoms removed per monomer during polymerization process). Among the two growth methods,[31] namely **sequential growth (SG)** and **quick growth (QG)** methods, we applied the SG method to generate a coarse-grained model of a random hyperbranched polymer by sequentially attaching a node at a random position that represents a monomer from a root node (Figure 2a). The degree of branching

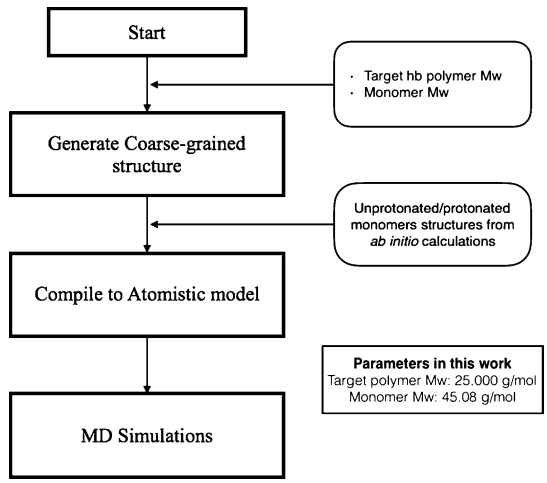

Figure 1. Schematic diagram of the strategy for generating the atomistic model of hyperbranched polymers.

$$\mathrm{DB} = \frac{2D}{2D + L}$$

is a useful parameter for characterizing hyperbranched structures. Here T, L, and D specify the number of terminal, linear, and dendritic units, respectively.[36] In order to obtain structures with the target degree of branching (0.5), we applied an additional constraint to the attachment probability parameter[37] p = 0.2, which indicates the ratio of the probability of introducing a new node to linear nodes (i.e., secondary amine) to terminal nodes (i.e., primary amine). In both cases we prohibit formation of cyclic rings. Once a model was generated, we evaluated the Wiener index[38] of the model to avoid a previously generated repetitive structure. WI is defined as the cumulative distance of all pairs of nodes within the coarse-grained model evaluated by the following expression

$$W = \frac{1}{2}\sum_{i=1}^{N}\sum_{j=1}^{j} d_{ij}$$

where d_{ij} is the number of bonds separating the nodes i and j of the model, counted along the shortest path between them.[26,38] WI is

DOI: 10.1021/acs.macromol.7b02573
Macromolecules 2018, 51, 2187−2194

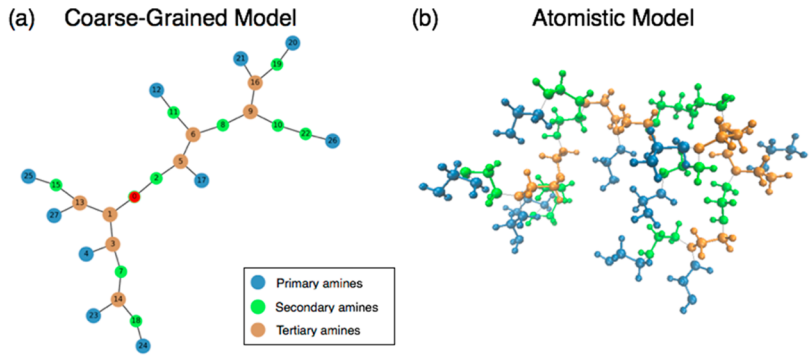

Figure 2. (a) Coarse-grained representation of a hyperbranched polymer with 28 monomers. The blue, green, and orange beads represent terminal, linear, and dendritic groups, respectively, and the red bead represents the root node. (b) Atomic structure of hyperbranched PEI built from a coarse-grained model in (a); the same color scheme is used.

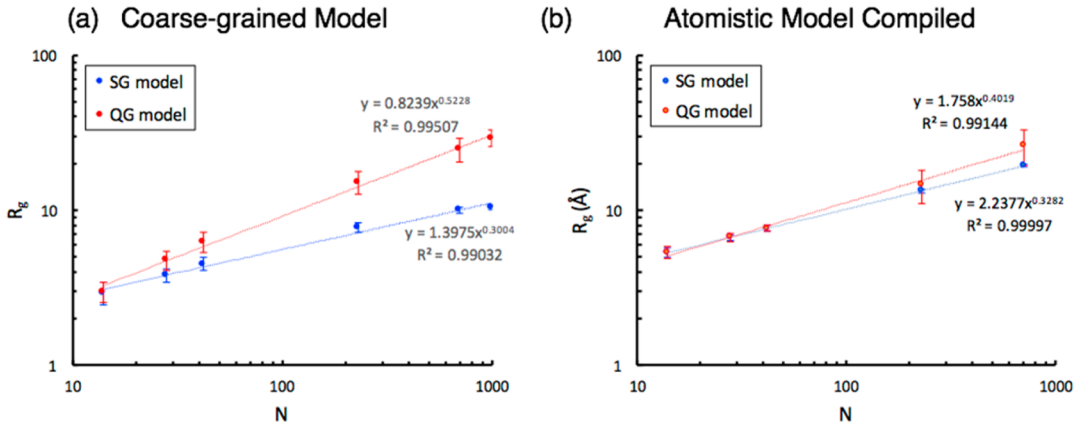

Figure 3. Power law behavior radius of gyration versus monomer number. (a) Coarse-grained model and (b) atomistic structure of hyperbranched PEI generated from the latter coarse-grained model which is equilibrated using gas-phase MD simulations.

calculated using the Networkx[39] package. At the end of this stage we have the coarse-grained structures for hyperbranched PEI (Figure 2b).

Next, we generated an atomistic structure for a randomly hyperbranched polymer based on the connectivity of nodes in the coarse-grained structure. First, the structure of an ethylamine monomer was prepared from Quantum Mechanics (QM) calculations using the B3LYP flavor of Density Functional Theory (DFT) with the 6-311+g* basis set using Q-Chem.[40] Partial charges were based on Mulliken charges of atoms consisting of primary, secondary, and tertiary amines. All monomers were sequentially appended one-by-one starting from the root node of the coarse-grained structure. When connecting two monomers, namely monomer A and B, a hydrogen atom on the amine group in the monomer A and a hydrogen atom in a methyl group in the monomer B are removed, and their partial charges are added to the connected atom in each monomer. The partial charge values we obtained from QM calculations and of our atomistic structure differed by less than 0.1 e. The structures were minimized to remove any artificial contacts at every attachment trial. After all monomers were connected, we used the Cohesive Energy Density (CED) annealing technique[41] to relax any strains in the molecular structure to achieve an equilibrated structure in gas phase.

Finally, we performed all-atom MD simulations of the atomistic hyperbranched PEI structures solvated in explicit water using LAMMPS.[42] Based on the experimental acid–base titration data,[21] we simulated ten model systems at three protonation levels:

- unprotonated case representing **basic pH** conditions (~ pH 10),
- all primary amines protonated representing **neutral pH** conditions (~ pH 7.8),
- and all primary and half of secondary amines protonated representing **low pH** conditions (~ pH 5.9).

The MD simulations were performed using the DREIDING III force field, which was used in previous PAMAM dendrimer simulations.[20] We used the F3C water model[43] to solvate hyperbranched PEI for all systems. Cl^- ions were added as counterions to neutralize the protonated systems. A 10 Å cutoff was used for van der Waals and real space electrostatics, with the van der Waals energies and forces tapered smoothly to zero from 9 Å using the seventh order taper function. 3D-Periodic boundary conditions were used, and the long-range electrostatics were evaluated using the PPPM[44] with a convergence tolerance of 10^{-4} kcal/mol.

The systems were simulated for 10 ns at 300 K with 1 fs time step and 1 atm pressure based on the isotropic NPT ensemble using the Nose-Hoover thermostat and barostat[45] with damping constants of 0.1 and 2.0 ps, respectively. The energy and temperature of the simulation box reached constant values during this process. The trajectories were recorded every 1 ps during 10 ns of the production run for analysis. In total, we performed 30 fully atomistic simulations.

3. RESULTS AND DISCUSSION

3.1. Growth Method. To find a suitable growth method for hyperbranched PEI, we generated a coarse-grained model using two methods, SG and QG. We also considered the perfect dendrimer structure for comparison. Figure S1 shows the relationship between DB and WI from SG and QG for various numbers of monomers. Without imposing the attachment probability parameter (meaning equal probability with $p = 0$), hyperbranched polymers built with the SG model have DB = 0.6 to 0.8, whereas polymers built with QG lead to DB ~ 0.5, indicating these methods induce different classes of hyperbranched structures. We observed that the DB value changes if the probability changes, and the DB converges to a specific value as the number of monomers N increases (Figure S2),

DOI: 10.1021/acs.macromol.7b02573
Macromolecules 2018, 51, 2187–2194

Table 1. Radius of Gyration, Asphericity δ, and the Aspect Ratio I_z/I_x,I_y/I_x, and I_z/I_y of Model Hyperbranched PEIs at Different pH Levels[b]

	experimental results[21]		this work				
pH	size (Å)	ellipticity	$\langle R_g \rangle$ (Å)	$\langle \delta \rangle$	$\langle I_z/I_x \rangle$	$\langle I_y/I_x \rangle$	$\langle I_z/I_y \rangle$
high pH	*a*	*a*	24 ± 1	0.037 ± 0.019	1.47 ± 0.17	1.27 ± 0.15	1.16 ± 0.06
neutral pH	22 ± 3	2	23 ± 1	0.030 ± 0.018	1.40 ± 0.16	1.23 ± 0.12	1.15 ± 0.07
low pH	20 ± 3	3	23 ± 2	0.068 ± 0.078	1.77 ± 0.82	1.60 ± 0.77	1.12 ± 0.06

[a]Not shown for clarity. [b]Experimental values are from Griffiths et al.[21]

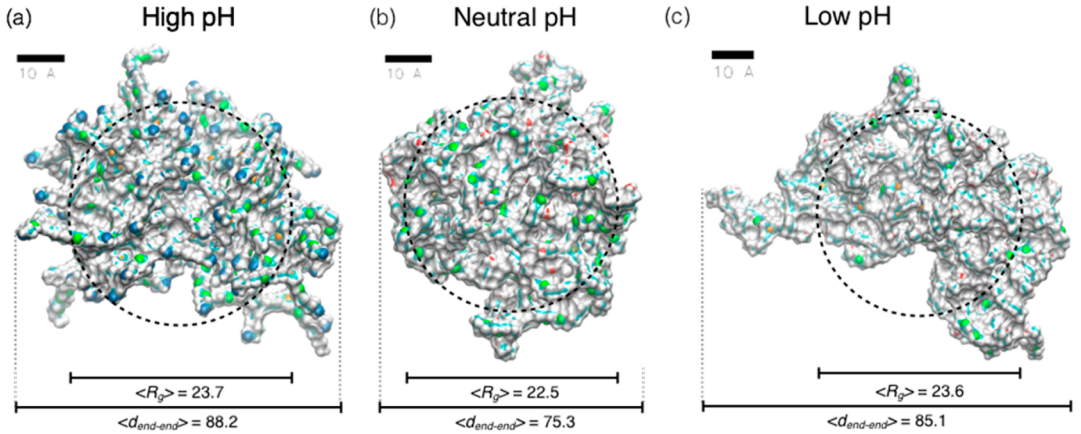

Figure 4. Snapshots of hyperbranched PEI under different pH conditions: (a) at high pH (~10), (b) at neutral pH (~7.8), and (c) at low pH (~5.9). The blue, green, and orange represent nitrogen atoms of primary, secondary, and tertiary amines, respectively. Protonated primary and secondary amines are colored as red. Values are averaged over 10 samples. Surface represents the solvent accessible surface with a probe radius 1.4 Å. Water molecules and counterions are not shown for clarity. The figures were generated using VMD.[49]

similar to the formula suggested by Schmidt and co-workers.[37] However, the behavior of the DB values does not agree with the formula for small N values. Figure S3 displays the behavior of the smallest eigenvalue λ_{min} of the connectivity matrix for the random structures created with the SG and QG models. In the double logarithmic representation, straight lines indicate that two methods generate polymer structures obeying power laws.[29,30] Using linear regression, we obtained the slopes for each growth method: −1.447 for the QG method, −1.104 for the SG method, and −1.037 for the dendrimer (fully branched). These values are in very close agreement with the values, −1.505 for the QG model, −1.031 for the SG model, and −1.027 for the dendrimer, reported by Jurjiu and co-workers.[31] Similar power values for the structures from the SG method and fully branched dendrimers indicate that structures from the SG method possess similar local branching properties to those of dendrimers.

Having obtained coarse-grained structures from two different growth methods, we generated atomistic structures of hyperbranched PEI and performed MD simulations to obtain the radius of gyration, R_g, for each atomistic hyperbranched PEI, defined by

$$R_g^2 = \frac{1}{M}\sum_i m_i(r_i - r_{cm})^2$$

where m_i is the mass of atom i, r_i is the position of atom i, and r_{cm} is the center of mass of hyperbranched polymers. Figure 3 uses a double-logarithmic scale to show the average R_g of hyperbranched PEI over the more than 100 samples generated by SG and QG methods. Surprisingly, the random hyperbranched structures obtained with both the SG and QG models lead to a straight line for the averaged R_g. Thus, they both obey a power law $R_g^2 \sim N^{\alpha}$. Moreover, SG showed a slightly better fit in the R_g value of the atomistic model. This supports the conclusion that for hyperbranched PEI, the SG method provides slightly more realistic atomistic structures than the QG method.

3.2. Radial Density Profiles and Conformations. Figure S4 shows the effect of pH on the average radial density for hyperbranched PEI. This parameter is measured from the center-of-mass of each sample and ensemble-averaged over 10 ns snapshots taken every 1 ps (total 10,000 snapshots). Although all samples possess a similar degree of branching, the monomers are randomly branched leading to different configurations. Radial density profiles of hyperbranched polymers are highly irregular unlike the case of dendrimers[20,46,47] or linear polymers;[16] therefore, there is the possibility of obtaining misleading results if the radial density values are simply averaged over all trajectories and samples. Nevertheless, some common features can be found from individual radial density profiles:

(1) slight increase of density for polymers is observed in the outer region (r > 15 Å) for neutral and low pH conditions indicating a dense-shell structure;

(2) sharp decrease of density is observed in the inner region (5 Å < r < 10 Å) indicating an enhanced internal shell structure at neutral pH condition;

(3) the density of water decreased for neutral and low pH conditions.

Again, it is worth mentioning that the radial density profile alone is not a robust metric to describe conformational changes of hyperbranched PEI.

To provide a better view on pH-responsive conformational changes, we investigated the shape of hyperbranched PEI in various pH conditions via calculating the gyration tensor I

DOI: 10.1021/acs.macromol.7b02573
Macromolecules 2018, 51, 2187−2194

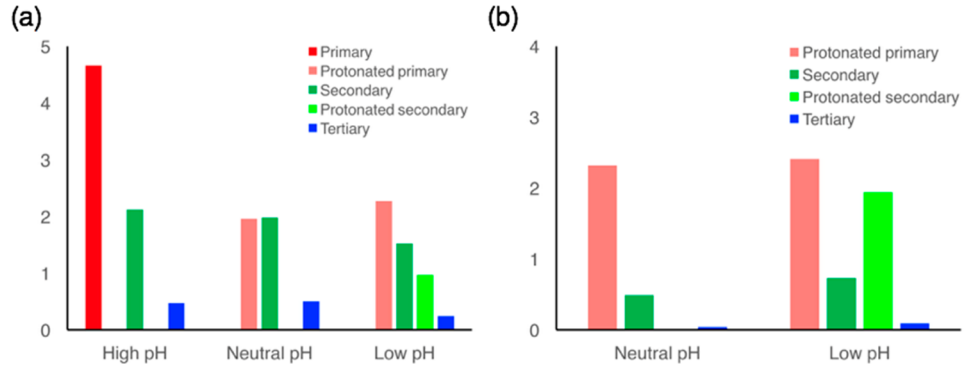

Figure 5. Coordination numbers at different pH levels of (a) water and (b) Cl^- ions around the amine N atoms.

$$I_{\alpha\beta} = \frac{1}{N}\left[\sum_{i=1}^{N}(r_{i,\alpha} - r_{\mathrm{cm},\alpha})(r_{i,\beta} - r_{\mathrm{cm},\beta})\right]$$

where $\alpha, \beta = x, y, z$, and asphericity δ[48]

$$\delta = \frac{1}{2}\cdot\frac{(I_x - I_y)^2 + (I_y - I_z)^2 + (I_x - I_z)^2}{I_x^2 + I_y^2 + I_z^2}$$

which takes values between 0 (spherical) and 1 (rodlike). Table 1 shows that the asphericity values vary from 0.037 to 0.068 as pH decreases, meaning that

- at high pH hyperbranched PEIs have spherelike conformations whereas
- at low pH the morphology is ellipsoidal or qualitatively elongated.

Although all values of δ are less than 0.10 and the difference between two states are subtle, there is a remarkable deviation in the aspect ratio. The aspect ratio of the three principal moments of inertia, I_z/I_x, I_y/I_x, *and* $I_z/I_y(I_x \le I_y \le I_z)$, represents relative shape, where spherical structures are closer to 1.0, while ellipsoid structures deviate from 1.0. Table 1 indicates that the aspect ratio I_z/I_x *and* I_y/I_x increases at low pH, meaning that it oblates along the third principal moments of inertia. This tendency to elongate is consistent with the result of SANS experiments,[21] which show that the ellipticity increases as pH decreases. Figure 4 presents representative snapshots from our MD simulations at high and low pH levels. Similar behavior is found experimentally in the pH-responsive conformation studies with linear PEI;[16] *the protonation of PEI induces elongation of the polymer structure*. Also, this change is consistent with the behavior of PAMAM dendrimers, which have a "dense-shell" structure with dense structure at the polymer periphery.[20]

3.3. Radial Distribution Functions and Coordination Numbers. The radial distribution function (RDF) gives the probability of finding an atom at a distance r from another atom, and the integral of the RDF up to the first minima calculates the first solvation shell coordination number. We analyzed the coordination numbers for water and counterions around each amine using the last 1 ns of the MD production run trajectory.

Radial distributions between the N atoms of the hyperbranched PEI and the oxygen (O) atoms of water molecules for various protonation states are depicted in Figure S5, and the coordination numbers are shown in Figure 5. Clear sharp peaks in Figure S5a show that the amine groups in hyperbranched PEI are hydrophilic under basic conditions. Since primary amines are protonated in neutral pH conditions, Cl^- ions bind to the N atom of two protonated primary amines (~2.32 Cl^- ions in the first solvation shell for protonated primary amines) so that the number of water molecules around each protonated primary amine decreases to 1.96. At low pH, there exist 2.41 Cl^- ions near each protonated primary amine and 1.94 near protonated secondary amines, indicating strong binding between hyperbranched PEI and Cl^- ions. This ultimately leads to denser structures that maximize the electrostatic interactions in acidic conditions.

3.4. Radius of Gyration. The conformational changes of charged PEI in solution can be investigated through the radius of gyration. R_g is calculated as an ensemble average over the 10 ns production runs and over sample molecules. Table 1 and Figure 4 show that there exist conformational changes along pH variations. In general, the R_g values calculated here at various pH conditions are in good agreement with the result from the SANS[21] experiments (Table 1), which are reported as ~25 Å. At high pH, all primary amines are freely pointing outward, thus the R_g value of primary amines is 23.7 Å, ~14% higher than that of overall amine groups (Figure S6). At neutral pH, the average R_g decreases with back-folding of the terminal groups, due to the increased electrostatic binding between PEI and Cl^- ions. However, at low pH, the R_g value for primary and secondary amines increases slightly, whereas that of tertiary amines remains the same, perhaps due to a binding of protonated amines with counter-anions in the outer shell region. Considering the SANS measurements were performed in nondilute conditions and the fitting model is different, one cannot compare the experimental result directly to our simulation results due to the possibility of aggregation between PEI polymers in high-pH conditions. Nevertheless, the overall trend on the elongation without much change in size shown in this simulation is consistent with the experimental observations. It is worth noticing that the inclusion of additional Na^+ ions, which mimics the experimental conditions, would decrease the amount of Cl^- ions associated with the PEI due to the competition with the PEI. This may lead to less dense structures with larger R_g values, as shown in the DNA 3-way junction simulations.[50]

3.5. Solvent Accessible Surface Area. Surface area is an important property for many applications of dendrimers and hyperbranched polymers, since most of the chemistry (binding and separations) occurs at the polymer surface. We calculated solvent-accessible surface area (SASA) using VMD.[49] The calculated results of SASA at various pH conditions with a probe radius 1.4 Å are tabulated in Table S1, and $SASA^{1/2}$ as functions of a probe radius r is plotted in Figure 6. We see that

DOI: 10.1021/acs.macromol.7b02573
Macromolecules 2018, 51, 2187−2194

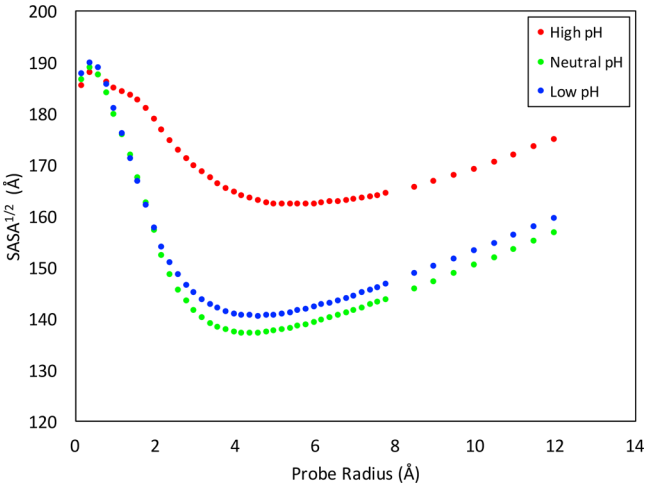

Figure 6. Square root of solvent accessible surface areas (SASA) as a function of the probe radius at high, neutral, and low pH. The decrease in SASA at neutral and low pH indicates a decrease of possibility for water molecules to access inside the hyperbranched PEI.

the solvent accessible surface area decreases drastically by 15.0% from high to low pH, assuming a probe radius of 1.4, consistent with the size of a water molecule. Figure 6 shows that the value of $SASA^{1/2}$ is proportional to the probe radius of $r > 6$ Å, indicating that only the exterior surface of the polymer is sampled and that molecules with a radius > 6 Å may not fit inside the polymer. At neutral pH the value of $SASA^{1/2}$ in the range of 2 Å < r < 3 Å is smaller than that of low pH, underscoring the increase in 2—3 Å cavities at low pH and indicating a transition from a dense-core to a dense-shell conformation. Additionally, the significant decrease of SASA in the low pH conformations for r < 4 Å indicates the decrease probability of water molecules accessing the hyperbranched polymers at low pH conditions in the densely packed regions.

4. CONCLUSIONS

We carried out all-atom molecular dynamics simulations on randomly hyperbranched PEI molecules with a molecular weight of 25 kDa and examined the pH-dependent conformational changes in aqueous solution. We employed a stepwise sequential growth method to build a coarse-grained model for monomer connectivity with specific degrees of the branching ratio, and then we converted to an all-atom polyamine polymer structure to obtain more realistic atomistic structures. From evaluating the asphericity and aspect ratio, we conclude that the conformations at low pH undergo oblate ellipsoidal elongation compared to high or neutral pH, which is consistent with results from small angle neutron scattering experiments. At low pH, we observe such structural changes as a decrease in size due to backfolding and a decrease in solvent accessible surface area due to electrostatic repulsions between protonated amine groups, which are both consistent with the behavior of dendrimers having well-defined structures. A future effort with the atomistic model will be the effect of competing salt buffer, electrostatic potential surface, and the behavior of anion binding of the hyperbranched PEI macromolecule. We expect that these results from the first fully atomistic MD study of hyperbranched PEI in solution will serve as a starting point for obtaining a deeper understanding of hyperbranched PEI and allow the current gap to be bridged between atomistic-level structures and experimental phenomena such as in gene delivery and membrane separations.

■ ASSOCIATED CONTENT

Supporting Information

The Supporting Information is available free of charge on the ACS Publications website at DOI: 10.1021/acs.macromol.7b02573.

DB values vs Wiener index from SG and QG growth models, Figure S1; attachment probability parameter compared to the DB value ranging from 0.0 to 3.0, Figure S2; behavior of the smallest eigenvalue of the connectivity matrix, Figure S3; averaged radial density profiles of all atoms on model hyperbranched PEIs, Figure S4; radial distribution functions for model hyperbranched PEIs between N of PEI and water and ions, Figure S5; radius of gyration of the N atoms in amine groups and all atoms, Figure S6; SASA and the effective outer radius R_{SASA} of model hyperbranched PEIs at different pH levels, Table S1 (PDF)

LAMMPS input and data files for 10 equilibrated structures of 25 kDa hyperbranched PEI (ZIP)

■ AUTHOR INFORMATION

Corresponding Authors

*E-mail: wag@wag.caltech.edu.
*E-mail: ysjn@kaist.ac.kr.

ORCID

In Kim: 0000-0002-2601-801X
Tod A. Pascal: 0000-0003-2096-1143
William A. Goddard III: 0000-0003-0097-5716
Yousung Jung: 0000-0003-2615-8394

Notes

The authors declare no competing financial interest.

■ ACKNOWLEDGMENTS

We acknowledge the generous support from the Climate Change Research Hub Project of the KAIST EEWS Research Center. WAG received partial support from DOE-STTR DE-SC0017710.

■ REFERENCES

(1) Gao, C.; Yan, D.; Frey, H. Promising Dendritic Materials: An Introduction to Hyperbranched Polymers. *Hyperbranched Polym. Synth. Prop. Appl.* **2011**, 1−26.

(2) Voit, B.; Komber, H.; Lederer, A. Hyperbranched Polymers: Synthesis and Characterization Aspects. *Mater. Sci. Technol.* **2013**, DOI: 10.1002/9783527603978.mst0434.

(3) Zheng, Y.; Li, S.; Weng, Z.; Gao, C. Hyperbranched Polymers: Advances from Synthesis to Applications. *Chem. Soc. Rev.* **2015**, *44* (12), 4091−4130.

(4) Jäger, M.; Schubert, S.; Ochrimenko, S.; Fischer, D.; Schubert, U. S. Branched and Linear Poly(ethylene Imine)-Based Conjugates: Synthetic Modification, Characterization, and Application. *Chem. Soc. Rev.* **2012**, *41* (13), 4755−4767.

(5) Pandey, A. P.; Sawant, K. K. Polyethylenimine: A Versatile, Multifunctional Non-Viral Vector for Nucleic Acid Delivery. *Mater. Sci. Eng., C* **2016**, *68*, 904−918.

(6) Sun, C.; Tang, T.; Uludağ, H.; Cuervo, J. E. Molecular Dynamics Simulations of DNA/PEI Complexes: Effect of PEI Branching and Protonation State. *Biophys. J.* **2011**, *100* (11), 2754−2763.

DOI: 10.1021/acs.macromol.7b02573
Macromolecules 2018, 51, 2187−2194

(7) Rivera-Tirado, E.; Wesdemiotis, C. Characterization of Polyethylenimine by Electrospray Ionization and Matrix-Assisted Laser Desorption/ionization. *J. Mass Spectrom.* **2011**, *46* (9), 876−883.
(8) Neu, M.; Fischer, D.; Kissel, T. Recent Advances in Rational Gene Transfer Vector Design Based on Poly(ethylene Imine) and Its Derivatives. *J. Gene Med.* **2005**, *7* (8), 992−1009.
(9) Mishra, H.; Yu, C.; Chen, D. P.; Goddard, W. a; Dalleska, N. F.; Hoffmann, M. R.; Diallo, M. S. Branched Polymeric Media: Boron-Chelating Resins from Hyperbranched Polyethylenimine. *Environ. Sci. Technol.* **2012**, *46* (16), 8998−9004.
(10) Chen, D. P.; Yu, C.; Chang, C.-Y.; Wan, Y.; Frechet, J. M. J.; Goddard, W. a; Diallo, M. S. Branched Polymeric Media: Perchlorate-Selective Resins from Hyperbranched Polyethyleneimine. *Environ. Sci. Technol.* **2012**, *46* (19), 10718−10726.
(11) Park, S.-J.; Cheedrala, R. K.; Diallo, M. S.; Kim, C.; Kim, I. S.; Goddard, W. a. Nanofiltration Membranes Based on Polyvinylidene Fluoride Nanofibrous Scaffolds and Crosslinked Polyethyleneimine Networks. *J. Nanopart. Res.* **2012**, *14* (7), 884.
(12) Sun, S. P.; Hatton, T. A.; Chung, T.-S. Hyperbranched Polyethyleneimine Induced Cross-Linking of Polyamide-Imide Nanofiltration Hollow Fiber Membranes for Effective Removal of Ciprofloxacin. *Environ. Sci. Technol.* **2011**, *45* (9), 4003−4009.
(13) Gao, J.; Sun, S.-P.; Zhu, W.-P.; Chung, T.-S. Polyethyleneimine (PEI) Cross-Linked P84 Nanofiltration (NF) Hollow Fiber Membranes for Pb2+ Removal. *J. Membr. Sci.* **2014**, *452*, 300−310.
(14) Curtis, K. A.; Miller, D.; Millard, P.; Basu, S.; Horkay, F.; Chandran, P. L. Unusual Salt and pH Induced Changes in Polyethylenimine Solutions. *PLoS One* **2016**, *11* (9), e0158147.
(15) Godbey, W. T.; Wu, K. K.; Mikos, A. G. Poly(ethylenimine) and Its Role in Gene Delivery. *J. Controlled Release* **1999**, *60* (2−3), 149−160.
(16) Choudhury, C. K.; Roy, S. Structural and Dynamical Properties of Polyethylenimine in Explicit Water at Different Protonation States: A Molecular Dynamics Study. *Soft Matter* **2013**, *9* (7), 2269.
(17) Neuberg, P.; Kichler, A. *Recent Developments in Nucleic Acid Delivery with Polyethylenimines*; Elsevier: 2014; Vol. *88*, DOI: 10.1016/B978-0-12-800148-6.00009-2.
(18) Zhao, C.; Nie, S.; Tang, M.; Sun, S. Polymeric pH-Sensitive membranes—A Review. *Prog. Polym. Sci.* **2011**, *36* (11), 1499−1520.
(19) Wang, N.; Zhang, G.; Ji, S.; Qin, Z.; Liu, Z. The Salt-, pH- and Oxidant-Responsive Pervaporation Behaviors of Weak Polyelectrolyte Multilayer Membranes. *J. Membr. Sci.* **2010**, *354* (1−2), 14−22.
(20) Liu, Y.; Bryantsev, V. S.; Diallo, M. S.; Goddard, W. A., III PAMAM Dendrimers Undergo pH Responsive Conformational Changes without Swelling. *J. Am. Chem. Soc.* **2009**, *131* (8), 2798−2799.
(21) Griffiths, P. C.; Paul, A.; Fallis, I. A.; Wellappili, C.; Murphy, D. M.; Jenkins, R.; Waters, S. J.; Nilmini, R.; Heenan, R. K.; King, S. M. Derivatizing Weak polyelectrolytes—Solution Properties, Self-Aggregation, and Association with Anionic Surfaces of Hydrophobically Modified Poly(ethylene Imine). *J. Colloid Interface Sci.* **2007**, *314* (2), 460−469.
(22) Mulder, T.; Lyulin, A. V.; van der Schoot, P.; Michels, M. A. J. Architecture and Conformation of Uncharged and Charged Hyperbranched Polymers: Computer Simulation and Mean-Field Theory. *Macromolecules* **2005**, *38* (3), 996−1006.
(23) Seiler, M. Hyperbranched Polymers: Phase Behavior and New Applications in the Field of Chemical Engineering. *Fluid Phase Equilib.* **2006**, *241* (1−2), 155−174.
(24) Aerts, J. Prediction of Intrinsic Viscosities of Dendritic, Hyperbranched and Branched Polymers. *Comput. Theor. Polym. Sci.* **1998**, *8* (1−2), 49−54.
(25) Widmann, A. H.; Davies, G. R. Simulation of the Intrinsic Viscosity of Hyperbranched Polymers with Varying Topology. 1. Dendritic Polymers Built by Sequential Addition. *Comput. Theor. Polym. Sci.* **1998**, *8* (1−2), 191−199.
(26) Sheridan, P. F.; Adolf, D. B.; Lyulin, A. V.; Neelov, I.; Davies, G. R. Computer Simulations of Hyperbranched Polymers: The Influence of the Wiener Index on the Intrinsic Viscosity and Radius of Gyration. *J. Chem. Phys.* **2002**, *117* (16), 7802.
(27) Konkolewicz, D.; Gray-Weale, A.; Perrier, S. Describing the Structure of a Randomly Hyperbranched Polymer. *Macromol. Theory Simul.* **2010**, *19* (5), 219−227.
(28) Galina, H.; Lechowicz, J. B.; Walczak, M. Kinetic Modeling of Hyperbranched Polymerization Involving an AB2Monomer Reacting with Substitution Effect. *Macromolecules* **2002**, *35* (8), 3253−3260.
(29) Buzza, D. M. a. Power Law Polydispersity and Fractal Structure of Hyperbranched Polymers. *Eur. Phys. J. E: Soft Matter Biol. Phys.* **2004**, *13* (1), 79−86.
(30) Richards, E. L.; Martin, D.; Buzza, A.; Davies, G. R. Monte Carlo Simulation of Random Branching in Hyperbranched Polymers. *Macromolecules* **2007**, *40* (6), 2210−2218.
(31) Jurjiu, A.; Dockhorn, R.; Mironova, O.; Sommer, J.-U. Two Universality Classes for Random Hyperbranched Polymers. *Soft Matter* **2014**, *10* (27), 4935−4946.
(32) Ziebarth, J. D.; Wang, Y. Understanding the Protonation Behavior of Linear Polyethylenimine in Solutions through Monte Carlo Simulations. *Biomacromolecules* **2010**, *11* (1), 29−38.
(33) Poghosyan, A. H.; Arsenyan, L. H.; Antonyan, L. A.; Shahinyan, A. A.; Koetz, J. Molecular Dynamics Simulations of Branched Polyethyleneimine in Water-in-Heptanol Micelles Stabilized by Zwitterionic Surfactants. *Colloids Surf., A* **2015**, *479*, 18−24.
(34) Von Harpe, A.; Petersen, H.; Li, Y.; Kissel, T. Characterization of Commercially Available and Synthesized Polyethylenimines for Gene Delivery. *J. Controlled Release* **2000**, *69* (2), 309−322.
(35) Girard, J. E.; Konaklieva, M.; Gu, J.; Guttman, C. M.; Wetzel, S. J. Characterization of Linear and Branched Polyethylenimine (PEI) by ESI-MS and MALDI-TOF-MS. *51st ASMS Conf. MAss Spectrom. Allied Top.* **2003**, 2−3.
(36) Frey, H.; Hölter, D. Degree of Branching in Hyperbranched Polymers. 3 Copolymerization of ABm-Monomers with AB and ABn-Monomers. *Acta Polym.* **1999**, *50* (2−3), 67−76.
(37) Schmidt, R.; Hernández Cifre, J.; de la Torre, J. Multi-Scale Simulation of Hyperbranched Polymers. *Polymers (Basel, Switz.)* **2015**, *7* (4), 610−628.
(38) Wiener, H. *J. Am. Chem. Soc.* **1947**, *69* (1), 17−20.
(39) Hagberg, A. A.; Schult, D. A.; Swart, P. J. Exploring Network Structure, Dynamics, and Function Using NetworkX. *Proc. 7th Python Sci. Conf.* **2008**, *836*, 11−15.
(40) Shao, Y.; Molnar, L. F.; Jung, Y.; Kussmann, J.; Ochsenfeld, C.; Brown, S. T.; Gilbert, A. T. B.; Slipchenko, L. V.; Levchenko, S. V.; O'Neill, D. P.; DiStasio, R. A.; Lochan, R. C.; Wang, T.; Beran, G. J. O.; Besley, N. A.; Herbert, J. M.; Lin, C. Y.; Van Voorhis, T.; Chien, S. H.; Sodt, A.; Steele, R. P.; Rassolov, V. A.; Maslen, P. E.; Korambath, P. P.; Adamson, R. D.; Austin, B.; Baker, J.; Byrd, E. F. C.; Dachsel, H.; Doerksen, R. J.; Dreuw, A.; Dunietz, B. D.; Dutoi, A. D.; Furlani, T. R.; Gwaltney, S. R.; Heyden, A.; Hirata, S.; Hsu, C.-P.; Kedziora, G.; Khalliulin, R. Z.; Klunzinger, P.; Lee, A. M.; Lee, M. S.; Liang, W.; Lotan, I.; Nair, N.; Peters, B.; Proynov, E. I.; Pieniazek, P. a; Rhee, Y. M.; Ritchie, J.; Rosta, E.; Sherrill, C. D.; Simmonett, A. C.; Subotnik, J. E.; Woodcock, H. L.; Zhang, W.; Bell, A. T.; Chakraborty, A. K.; Chipman, D. M.; Keil, F. J.; Warshel, A.; Hehre, W. J.; Schaefer, H. F.; Kong, J.; Krylov, A. I.; Gill, P. M. W.; Head-Gordon, M. Advances in Methods and Algorithms in a Modern Quantum Chemistry Program Package. *Phys. Chem. Chem. Phys.* **2006**, *8* (27), 3172−3191.
(41) Belmares, M.; Blanco, M.; Goddard, W. A.; Ross, R. B.; Caldwell, G.; Chou, S. H.; Pham, J.; Olofson, P. M.; Thomas, C. Hildebrand and Hansen Solubility Parameters from Molecular Dynamics with Applications to Electronic Nose Polymer Sensors. *J. Comput. Chem.* **2004**, *25* (15), 1814−1826.
(42) Plimpton, S. Fast Parallel Algorithms for Short-Range Molecular Dynamics. *J. Comput. Phys.* **1995**, *117* (1), 1−19.
(43) Levitt, M.; Hirshberg, M.; Sharon, R.; Laidig, K. E.; Daggett, V. Calibration and Testing of a Water Model for Simulation of the Molecular Dynamics of Proteins and Nucleic Acids in Solution. *J. Phys. Chem. B* **1997**, *101* (25), 5051−5061.

DOI: 10.1021/acs.macromol.7b02573
Macromolecules 2018, 51, 2187−2194

(44) Hockney, R.; Eastwood, J. *Computer Simulation Using Particles*; CRC Press: 1988.
(45) Shi, B.; Sinha, S.; Dhir, V. K.; Vázquez, U. O. M.; Shinoda, W.; Moore, P. B.; Chiu, C. C.; Nielsen, S. O. Molecular Dynamics Simulation of the Density and Surface Tension of Water by Particle-Particle Particle-Mesh Method. *J. Chem. Phys.* **2006**, *124* (20), 204715.
(46) Maiti, P. K.; Çağın, T.; Lin, S.-T.; Goddard, W. A. Effect of Solvent and pH on the Structure of PAMAM Dendrimers. *Macromolecules* **2005**, *38* (3), 979−991.
(47) Wu, C. PH Response of Conformation of Poly(propylene Imine) Dendrimer in Water: A Molecular Simulation Study. *Mol. Simul.* **2010**, *36* (14), 1164−1172.
(48) Todeschini, R.; Consonni, V. Descriptors from Molecular Geometry. In *Handbook of Chemoinformatics*; Wiley-VCH Verlag GmbH: Weinheim, Germany, 2008; pp 1004−1033, DOI: 10.1002/9783527618279.ch37.
(49) Humphrey, W.; Dalke, A; Schulten, K. VMD: Visual Molecular Dynamics. *J. Mol. Graphics* **1996**, *14* (1), 33−38 27−28..
(50) Pascal, T. A.; Goddard, W. A.; Maiti, P. K.; Vaidehi, N. Role of Specific Cations and Water Entropy on the Stability of Branched DNA Motif Structures. *J. Phys. Chem. B* **2012**, *116* (40), 12159−12167.

DOI: 10.1021/acs.macromol.7b02573
Macromolecules 2018, 51, 2187−2194